

E14-2006-59

A. Loose¹, K. Wozniak², P. Dominiak², L. S. Smirnov^{3,4},
I. Natkaniec^{4,5}, M. V. Frontasyeva⁴, E. V. Pomjakushina⁴,
A. I. Baranov⁶, V. V. Dolbinina⁶

X-RAY AND NEUTRON SINGLE-CRYSTAL
DIFFRACTION ON $[\text{Rb}_x(\text{NH}_4)_{1-x}]_3\text{H}(\text{SO}_4)_2$
I. REFINEMENT OF CRYSTAL STRUCTURE OF
PHASE II WITH $x = 0.11$ AT 300 K

Submitted to «Crystallography»

¹ Hahn–Meitner Institute, BENSC, Berlin, Germany

² University of Warsaw, Warsaw, Poland

³ SSC RF Institute of Theoretical and Experimental Physics, Moscow, Russia

⁴ Frank Laboratory of Neutron Physics, Joint Institute for Nuclear Research,
Dubna, Russia

⁵ H. Niewodniczanski Institute of Nuclear Physics, Krakow, Poland

⁶ Shubnikov Institute of Crystallography RAS, Moscow, Russia

Лоозе А. и др. E14-2006-59
Рентгеновская и нейтронная дифракция на монокристалле
 $[\text{Rb}_x(\text{NH}_4)_{1-x}]_3\text{H}(\text{SO}_4)_2$. I. Уточнение кристаллической структуры
фазы II с $x = 0,11$ при 300 К

Результаты исследования смешанных кристаллов $[\text{Rb}_x(\text{NH}_4)_{1-x}]_3\text{H}(\text{SO}_4)_2$ методом рентгеновской дифракции на монокристалле известны до сих пор только для $x = 0,57$ при температурах 293 и 180 К. Кристаллические структуры при этих температурах, как было определено [1], принадлежат монокристаллической фазе II (пр. гр. $C2/c$, $Z = 4$). В соответствии с этой работой ионы аммония следовало бы рассматривать как деформированные тетраэдры. Моноклинная фаза II на x - T фазовой диаграмме смешанных кристаллов $[\text{Rb}_x(\text{NH}_4)_{1-x}]_3\text{H}(\text{SO}_4)_2$, которая ранее была определена с помощью диэлектрической спектроскопии, стабилизируется ниже комнатной температуры, если концентрация Rb превосходит 9%. Представленные результаты рентгеновской и нейтронной монокристаллической дифракции смешанного кристалла $[\text{Rb}_{0.11}(\text{NH}_4)_{0.89}]_3\text{H}(\text{SO}_4)_2$ при $T = 300$ К показывают, что ионы аммония следовало бы рассматривать как регулярные тетраэдры.

Работа выполнена в Лаборатории нейтронной физики им. И. М. Франка ОИЯИ.

Препринт Объединенного института ядерных исследований. Дубна, 2006

Loose A. et al. E14-2006-59
X-Ray and Neutron Single-Crystal Diffraction on $[\text{Rb}_x(\text{NH}_4)_{1-x}]_3\text{H}(\text{SO}_4)_2$.
I. Refinement of Crystal Structure of Phase II with $x = 0.11$ at 300 K

The study of $[\text{Rb}_x(\text{NH}_4)_{1-x}]_3\text{H}(\text{SO}_4)_2$ mixed crystals by X-ray single-crystal diffraction is known up to now only for $x = 0.57$ at the temperatures 293 and 180 K. The crystal structures at these temperatures as was determined [1] belong to monoclinic phase II ($C2/c$ sp. gr., $Z = 4$). In accordance with this work, ammonium ions should be considered as deformed tetrahedra. Monoclinic phase II on the x - T phase diagram of $[\text{Rb}_x(\text{NH}_4)_{1-x}]_3\text{H}(\text{SO}_4)_2$ mixed crystals, which has earlier been determined by the dielectric spectroscopy, is stabilized below room temperature if Rb concentration exceeds 9%. The presented results of X-ray and neutron single-crystal diffraction of the $[\text{Rb}_{0.11}(\text{NH}_4)_{0.89}]_3\text{H}(\text{SO}_4)_2$ mixed crystal at $T = 300$ K show that ammonium ions could be considered as regular tetrahedra.

The investigation has been performed at the Frank Laboratory of Neutron Physics, JINR.

Preprint of the Joint Institute for Nuclear Research. Dubna, 2006

INTRODUCTION

The $(\text{NH}_4)_3\text{H}(\text{SO}_4)_2$ is a member of the $\text{Me}_3\text{H}(\text{SO}_4)_2$ family ($\text{Me} = \text{Na}, \text{K}, \text{Rb}, \text{Cs}, \text{NH}_4$), which is characterized by high temperature phase I with superionic conductivity. Then $(\text{NH}_4)_3\text{H}(\text{SO}_4)_2$ undergoes a series of phase transitions to phases II, III, IV, V and VII, which can be associated with the behaviour of NH_4^+ ions.

The crystal structure of trirubidium hydrogen disulfate-triammonium hydrogen disulfate ($[\text{Rb}_x(\text{NH}_4)_{1-x}]_3\text{H}(\text{SO}_4)_2$, or TRAHS) with rubidium concentration $x = 0.57$ was studied by X-ray single-crystal diffraction [1]. It was shown that at room temperature and at 180 K the crystal structures are isostructural and belong to the monoclinic system with $C2/c$ sp. gr., or to phase II; the unit cell contains two crystallographically non-equivalent ammonium groups $\text{NH}_4(1)$ and $\text{NH}_4(2)$. There are eight $\text{NH}_4(1)$ ions at general positions and four $\text{NH}_4(2)$ ions at special positions along twofold axes [2]. The determined hydrogen bond distances are different from an ideal tetrahedron. So N(1)–H hydrogen bond distances for $\text{NH}_4(1)$ were found in the range of 0.873(2)–0.984(2) Å and for $\text{NH}_4(2)$ in the range of 0.804(1)–0.858(1) Å. The results of X-ray single-crystal diffraction [1] did not determine an orientational order of ammonium ions in phase II of TRAHS.

The x – T phase diagram of the $[\text{Rb}_x(\text{NH}_4)_{1-x}]_3\text{H}(\text{SO}_4)_2$ mixed crystals, determined by dielectric spectroscopy [3], is presented in Fig. 1. The x – T phase diagram of these mixed crystals established the location of the bounds between different phases as a function of rubidium concentration in the whole concentration range of rubidium in the temperature interval from 500 up to 5 K. The mixed crystal with $x = 0.57$ at 293 and 180 K was indeed found in phase II, confirming the result [1].

The substitution of ammonium ions by Rb^+ ions significantly changes the series of phase transitions in $(\text{NH}_4)_3\text{H}(\text{SO}_4)_2$ already at $x > 9\%$. If high temperature phase transition from phase I to phase II is saved, and increasing of Rb concentration is accompanied by increasing of the temperature at this phase transition, then the situation is different below room temperature. At rubidium concentration, exceeding 9%, phase transitions $\text{II} \leftrightarrow \text{III}$, $\text{III} \leftrightarrow \text{IV}$, $\text{IV} \leftrightarrow \text{V}$ and $\text{V} \leftrightarrow \text{VII}$ are not observed, and only phase II is saved and the phase transition from phase II to orientation glass state is observed at cooling below 30 K.

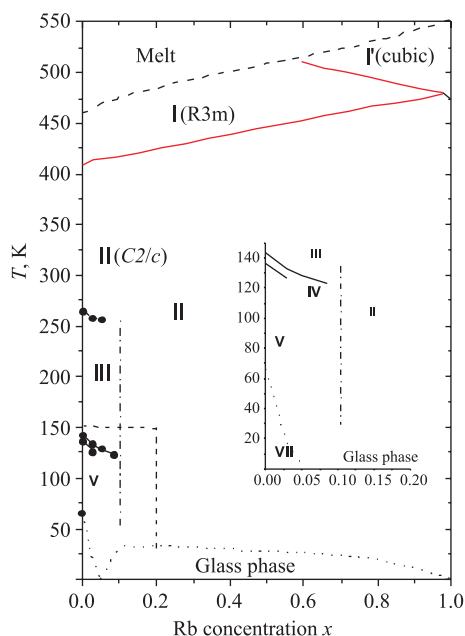


Fig. 1. The x - T phase diagram of the $[\text{Rb}_x(\text{NH}_4)_{1-x}]_3\text{H}(\text{SO}_4)_2$ mixed crystals

The presented study is dedicated to the refinement of crystal structure of the $[\text{Rb}_{0.11}(\text{NH}_4)_{0.89}]_3\text{H}(\text{SO}_4)_2$ mixed crystal by X-ray and neutron single-crystal diffraction to determine hydrogen bond lengths for $\text{NH}_4(1)$ and $\text{NH}_4(2)$ ammonium groups and the orientational order of these ammonium groups in phase II.

EXPERIMENTAL RESULTS AND DISCUSSION

The single crystal of the $[\text{Rb}_{0.11}(\text{NH}_4)_{0.89}]_3\text{H}(\text{SO}_4)_2$ mixed crystal has been prepared by evaporation of aqueous solution, and Rb concentration of the grown single crystal is determined by neutron activation analysis [4]. X-ray single-crystal diffraction measurements have been performed at room temperature using the Kuma4CCD X-ray diffractometer (Warsaw University, Chemistry Department, Poland) [5] and neutron single-crystal diffraction measurements have been carried out at room temperature on the E5 neutron four-circle diffractometer set on the BER-2 reactor of BENSC HMI (Berlin, Germany) [6].

The conditions of the measurements including the used wavelengths, the refined space group, the obtained lattice parameters, the number of measured

reflections, the number of unique reflections for the refinement of atomic positions and the R -factors of refinement are presented in Table 1.

Table 1. Experimental conditions of crystal structure refinement of the $[\text{Rb}_{0.11}(\text{NH}_4)_{0.89}]_3\text{H}(\text{SO}_4)_2$ mixed crystal at room temperature by neutron and X-ray single-crystal diffraction

Parameters	Neutron	X-ray
Wavelength	0.8902 Å	0.71073 Å
Space group, Z	$C2/c$, 4	$C2/c$, 4
a	15.261(3) Å	15.261(3) Å
b	5.8027(12) Å	5.8027(12) Å
c	10.065(2) Å	10.065(2) Å
α	90°	90°
β	101.81(3)°	101.81(3)°
γ	90°	90° _y
Volume	872.5(3) Å ³	872.5(3) Å ³
Data / restraints / parameters	1622 / 3 / 128	1085 / 3 / 65
Goodness-of-fit on F^2	1.180	1.118
Final R indices [$I > 2 \sigma(I)$]/ $R1/wR2$	0.1206/0.2547	0.0594/0.1847
R indices (all data)/ $R1/wR2$	0.1748/0.2840	0.0652/0.1969
Extinction coefficient	0.26(3)	0.119(13)
Largest diff. peak and hole	(1.437 and -1.323)·e. Å ⁻³	(0.599 and -0.912)·e. Å ⁻³

The atomic positions and equivalent isotropic displacement parameters U (eq), determined by means of neutron and X-ray single-crystal diffraction, are presented in Tables 2 and 3, respectively.

The U_{ij} anisotropic displacement parameters, determined by neutron and X-ray single-crystal diffraction, are presented in Tables 4 and 5, respectively.

The hydrogen positions in the $[\text{Rb}_{0.11}(\text{NH}_4)_{0.89}]_3\text{H}(\text{SO}_4)_2$ mixed crystal and U_{ij} hydrogen anisotropic displacement parameters are determined only with the help of neutron single-crystal diffraction. The projection of $[\text{Rb}_{0.11}(\text{NH}_4)_{0.89}]_3\text{H}(\text{SO}_4)_2$ mixed crystal to (010) plane is presented in Fig. 2. There one can see SO_4 -H- SO_4 dimers and ammonium ions, filling the unit cell.

The anisotropic thermal parameters depicted as thermal ellipsoids for atoms of N, S, O, and H are presented in Fig. 3. It is worth to note that the thermal parameters for H1 and H3 of $\text{NH}_4(1)$ ammonium group are significantly higher than those for H2 and H4, thermal parameter for H5 is higher than for H6 in $\text{NH}_4(2)$ ammonium group and this situation is imaged by thermal ellipsoids of

Table 2. Atomic coordinates ($\times 10^4$) and U (eq) equivalent isotropic displacement parameters ($\text{\AA}^2 \cdot 10^3$) defined as 1/3 of the trace of the orthogonalized Uij tensor (for X-ray data)

Neutron				
Atoms	<i>x</i>	<i>y</i>	<i>z</i>	U(eq)
S(1)	1142(4)	2177(9)	4627(6)	20(1)
O(1)	145(2)	1846(8)	4424(5)	37(1)
O(2)	1503(3)	2231(8)	6058(4)	39(1)
O(3)	1289(3)	4328(7)	3981(5)	41(1)
O(4)	1490(3)	273(7)	3982(5)	40(1)
Rb(1)	3012(2)	7757(4)	3471(2)	32(1)
N(1)	3012(2)	7757(4)	3471(2)	32(1)
Rb(2)	5000	2305(5)	2500	28(1)
N(2)	5000	2305(5)	2500	28(1)
H(1)	3277(15)	8970(40)	4050(30)	127(9)
H(2)	2380(10)	8190(40)	3330(30)	117(8)
H(3)	3198(15)	7860(40)	2630(16)	112(7)
H(4)	3108(11)	6260(30)	3870(20)	98(6)
H(5)	4589(18)	3140(60)	2760(40)	178(17)
H(6)	4651(11)	1290(30)	1816(17)	93(5)
H(10)	-43(14)	400(40)	130(20)	45(5)

Table 3. Atomic coordinates ($\times 10^4$) and U (eq) equivalent isotropic displacement parameters ($\text{\AA}^2 \cdot 10^3$), defined as 1/3 of the trace of the orthogonalized Uij tensor (for X-ray data)

X-ray				
Atoms	<i>x</i>	<i>y</i>	<i>z</i>	U(eq)
S(1)	1141(1)	2187(1)	4613(1)	28(1)
O(1)	143(2)	1840(5)	4430(3)	44(1)
O(2)	1503(2)	2233(5)	6052(3)	45(1)
O(3)	1291(2)	4340(5)	3982(3)	48(1)
O(4)	1491(2)	259(5)	3982(3)	47(1)
Rb(1)	3012(2)	7728(4)	3473(2)	65(1)
N(1)	3012(2)	7728(4)	3473(2)	65(1)
Rb(2)	5000	2324(5)	2500	49(1)
N(2)	5000	2324(5)	2500	49(1)

Table 4. The Uij anisotropic displacement parameters ($\text{\AA}^2 \cdot 10^3$) for neutron data

Atom	U11	U22	U33	U23	U13	U12
S	23(2)	18(2)	21(2)	0(2)	7(2)	4(2)
O1	20(1)	49(2)	41(2)	-1(2)	4(1)	4(1)
O2	35(2)	57(2)	22(2)	0(1)	2(1)	-7(2)
O3	43(2)	31(2)	47(2)	19(2)	7(2)	1(1)
O4	40(2)	32(2)	53(2)	-15(2)	20(2)	3(1)
Rb(1)	41(1)	28(1)	27(1)	0(1)	7(1)	7(1)
N(1)	41(1)	28(1)	27(1)	0(1)	7(1)	7(1)
Rb(2)	29(1)	32(1)	22(1)	0	5(1)	0
N(2)	29(1)	32(1)	22(1)	0	5(1)	0
H1	123(14)	108(13)	150(20)	-97(15)	36(13)	-34(11)
H2	61(7)	128(14)	170(20)	76(14)	34(9)	43(9)
H3	117(12)	180(20)	49(7)	0(8)	45(8)	30(12)
H4	89(9)	62(7)	134(14)	60(9)	1(8)	11(6)
H5	113(15)	180(30)	230(40)	-140(30)	16(18)	51(16)
H6	88(9)	97(10)	77(9)	-49(8)	-22(7)	10(8)
H1O	27(6)	69(18)	42(10)	10(10)	15(5)	22(8)

Table 5. The Uij anisotropic displacement parameters ($\text{\AA}^2 \cdot 10^3$) for X-ray data

Atom	U11	U22	U33	U23	U13	U12
S	30(1)	28(1)	26(1)	0(1)	6(1)	3(1)
O1	27(1)	58(2)	47(1)	-4(1)	6(1)	2(1)
O2	44(2)	63(2)	26(1)	1(1)	2(1)	-7(1)
O3	51(2)	37(1)	54(2)	18(1)	8(1)	2(1)
O4	44(1)	40(1)	63(2)	-17(1)	21(1)	2(1)
Rb(1)	77(2)	61(2)	58(2)	-1(1)	17(1)	8(1)
N(1)	77(2)	61(2)	58(2)	-1(1)	17(1)	8(1)
Rb(2)	47(2)	56(2)	43(2)	0	9(1)	0
N(2)	47(2)	56(2)	43(2)	0	9(1)	0

these hydrogen atoms. The acid hydrogens, allocated in a double-well potential in hydrogen bond O-H...O of the $\text{SO}_4\text{-H-SO}_4$ dimers, have distinguishable thermal parameters as it is imaged by their thermal ellipsoids.

The results of the determination of bond lengths [\AA] and angles [deg] from X-ray and neutron diffraction for ammonium and sulfate ions are presented in Table 6.

The S-O1 bond is predominant in the SO_4^{2-} tetrahedron in comparison with other bonds (S-Oj, where $j = 2, 3, 4$) and this peculiarity originates due to

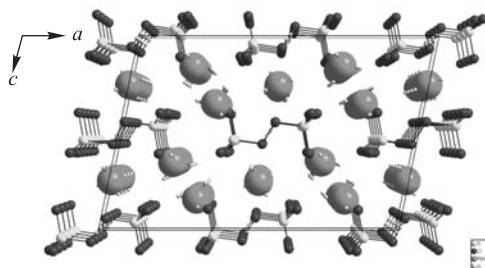


Fig. 2. The projection of $[\text{Rb}_{0.11}(\text{NH}_4)_{0.89}]_3\text{H}(\text{SO}_4)_2$ (at room temperature, $C2/c$ sp. gr.) along the Y axis – direction $[010]$

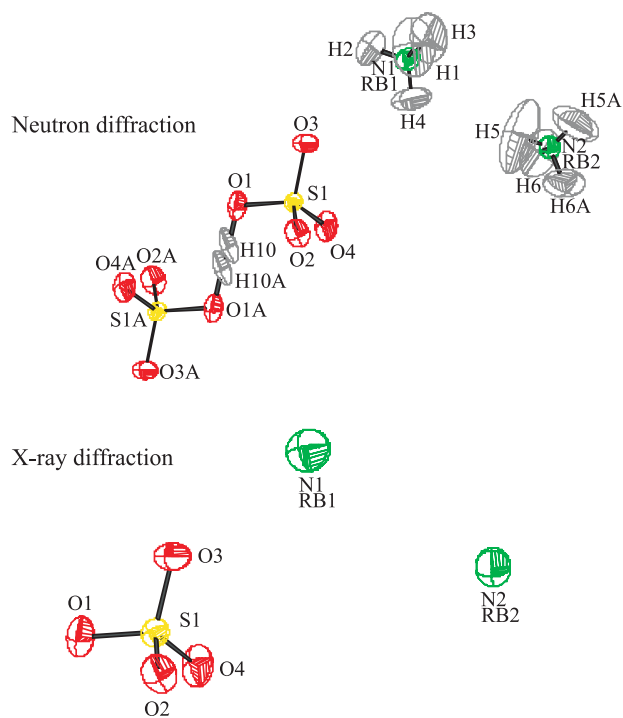


Fig. 3. The ellipsoids of anisotropic thermal parameters of the $[\text{Rb}_{0.11}(\text{NH}_4)_{0.89}]_3\text{H}(\text{SO}_4)_2$ mixed crystal for ammonium ions $\text{NH}_4(1)$ and $\text{NH}_4(2)$ and dimer $(\text{SO}_4)\text{H}(\text{SO}_4)$, $C2/c$ sp. gr., $Z = 4$, at room temperature

participation of O1 in the formation of the $(\text{SO}_4^{2-})\text{H}(\text{SO}_4^{2-})$ dimer. The values of S-O1 bond, determined by X-ray and neutron diffraction, are similar: 1.510(3)

Table 6. The results of the determination of bond lengths [Å] and angles [deg] from X-ray and neutron diffraction

Bond lengths [Å]	X-ray diffraction	Neutron diffraction
S(1)-O(1)	1.510(3)	1.507(7)
S(1)-O(2)	1.441(3)	1.434(7)
S(1)-O(3)	1.441(2)	1.445(6)
S(1)-O(4)	1.442(2)	1.437(6)
N(1)/Rb(1)-H(1)		0.950(13)
N(1)/Rb(1)-H(2)		0.978(13)
N(1)/Rb(1)-H(3)		0.948(13)
N(1)/Rb(1)-H(4)		0.952(10)
N(2)/Rb(2)-H(5)		0.874(19)
N(2)/Rb(2)-H(6)		0.977(12)
Angles [deg]		
O(2)-S(1)-O(3)	111.35(16)	111.7(5)
O(2)-S(1)-O(4)	110.91(17)	111.7(5)
O(3)-S(1)-O(4)	111.84(17)	110.8(5)
O(2)-S(1)-O(1)	107.11(17)	108.0(4)
O(3)-S(1)-O(1)	108.03(16)	107.1(4)
O(4)-S(1)-O(1)	107.35(16)	107.3(4)
H(1)- N(1)/Rb(1)-H(2)		101(2)
H(1)- N(1)/Rb(1)-H(3)		109(2)
H(2)- N(1)/Rb(1)-H(3)		109(2)
H(1)- N(1)/Rb(1)-H(4)		114(3)
H(2)- N(1)/Rb(1)-H(4)		111.1(15)
H(3)- N(1)/Rb(1)-H(4)		112(2)
H(5)- N(2)/Rb(2)-H(6)		103(2)

and 1.507(7) Å, respectively, and the averages of other S-O_j (j = 2, . . . 4) bonds, also determined by X-ray and neutron diffraction, are equal to 1.441(2) and 1.439(6) Å, respectively.

The N-H bonds for ammonium groups NH₄(1)/Rb(1) and NH₄(2)/Rb(2), determined by X-ray diffraction in [1] and presented by recent neutron diffraction, have the following relations: for NH₄(1)/Rb(1) the average N-H bonds have 0.948(2) and 0.957(12) Å, respectively, and for NH₄(2)/Rb(2) the average N-H bonds have 0.837(1) and 0.923(15) Å, respectively. The N-H bonds, obtained in the result of an averaging over N(i)-H(j) (i = 1, 2 and j = 1, . . . 6) of NH₄(1)/Rb(1) and NH₄(2)/Rb(2) groups, determined by X-ray in [1] and by recent neutron diffraction, have average values 0.890(2) and 0.940(13) Å, respectively. Thus, one may conclude that the ammonium ions could be presented by regular tetrahedra.

The distinctive feature between N-H bonds, obtained by X-ray diffraction and by neutron diffraction, is due to the distribution of electron charge density of ammonium ions in the crystal lattice, reproducing the formation of chemical connection in this molecular-ionic compound.

In future we shall use the presentation of the electron charge density, obtained from X-ray diffraction experimental data, and nuclear hydrogen density, obtained from neutron diffraction experimental data, with the help of Fourier maps or with the help of differential Fourier maps (DFM) [7]. The differential Fourier map is Fo-Fc, where Fo is experimental structure factor and Fc is calculated structural factor. The 2Fo-Fc differential Fourier map is used to reveal the delicacies in distribution of the electron charge densities or nuclear densities (hydrogen atoms).

The comparison of the electron density map of the (SO₄)-H(10)-(SO₄) dimer with that of nuclear density is presented in Fig. 4 as Fo-Fc DFM and 2Fo-Fc DFM, obtained from X-ray diffraction data and neutron diffraction data, respectively. These DFM present the hydrogen distribution along O1-H(10)...O1A hydrogen

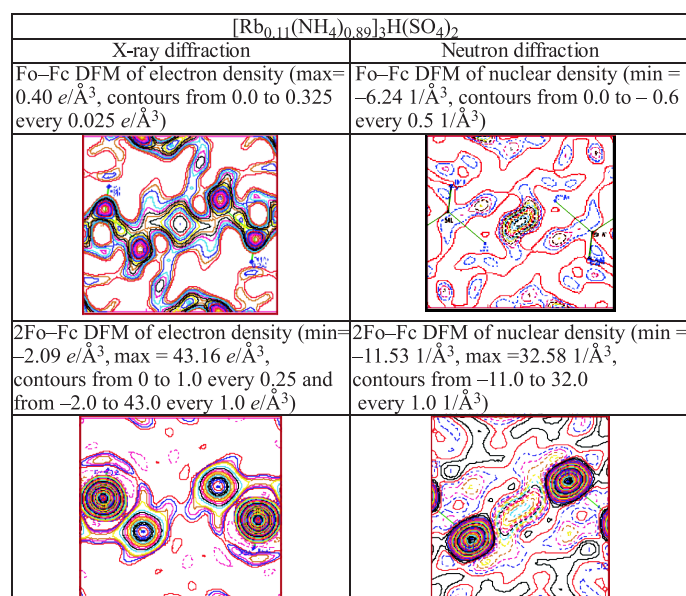


Fig. 4. Fourier maps in the region of the H(10) atom in the S(1)O(1)HS(1A)O(1A) plane where the label *A* stands for atoms related to a symmetry centre for (SO₄)-H-(SO₄) dimer

bond of the (SO₄)-H(10)-(SO₄) dimer. The 2Fo-Fc DFM of electron density presents the distribution of hydrogen charge along O1-H(10)...O1A hydrogen

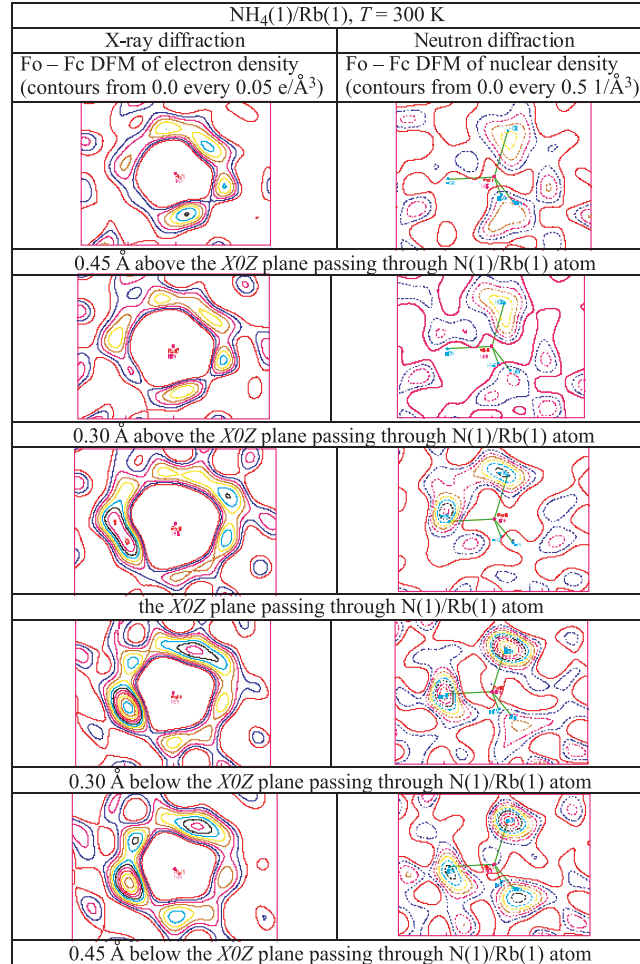


Fig. 5. The Fo-Fc DFM of electron density and nuclear density near NH₄(1)/Rb(1) group

bond as two additional maximal electron densities near O1 and O1A oxygen atoms. This picture confirms the result, obtained in [1], and shows, that in phase II H(1O) acid hydrogen occupies two positions with equal probability (50 %) along O1-H(1O)...O1A hydrogen bond. On the other hand, Fo-Fc and 2Fo-Fc DFM of nuclear density also show that hydrogen atom occupies two different statistically well-defined positions with an equal probability (50 %) along the O1-H(1O)...O1A hydrogen bond.

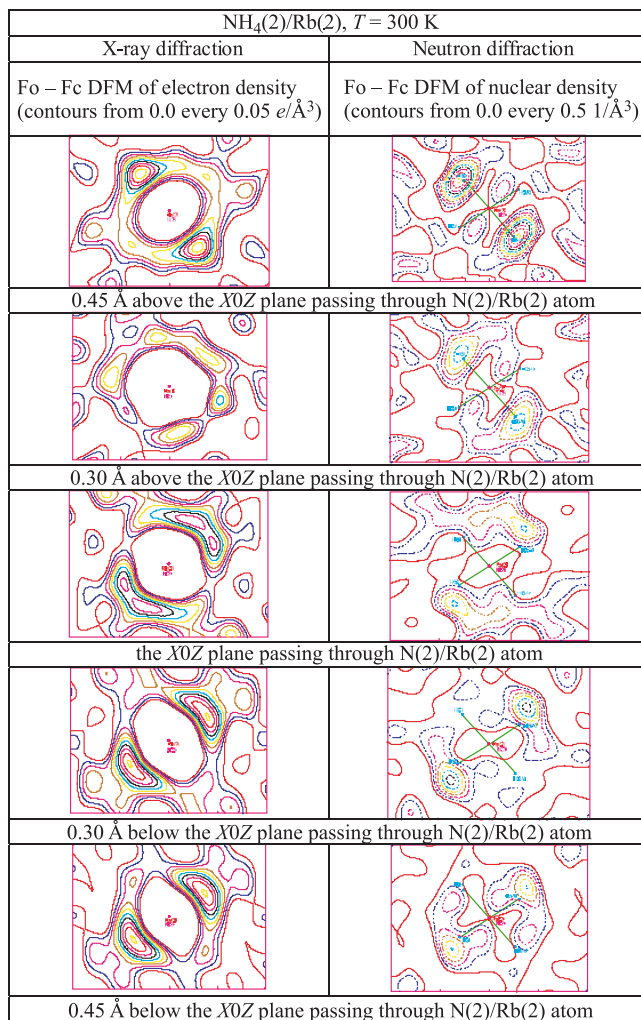


Fig. 6. The Fo-Fc DFM of electron density and nuclear density near NH₄(2)/Rb(2) group

The Fo-Fc DFM of electron densities and the Fo-Fc DFM of nuclear densities for NH₄(1) and NH₄(2) groups are presented in Figs. 5 and 6, respectively, in order to better understand orientational positions of ammonium groups.

The Fo-Fc DFM of electron density and the Fo-Fc DFM of nuclear density for NH₄(1) are numerical and shifted above or below the N1_010 zero plane, for example, at 0.45 and 0.30 Å above the X0Z plane passing through N(1)/Rb(1) atom. These Fo-Fc DFM could be used to localize positions of particular H-atoms

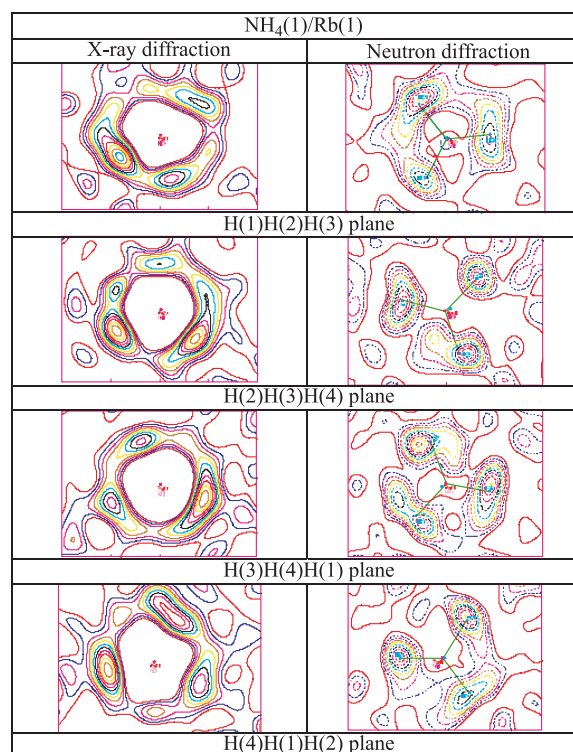


Fig. 7. The Fo-Fc DFM of electron density and nuclear density near NH₄(1)/Rb(1) group in HiHkHj planes

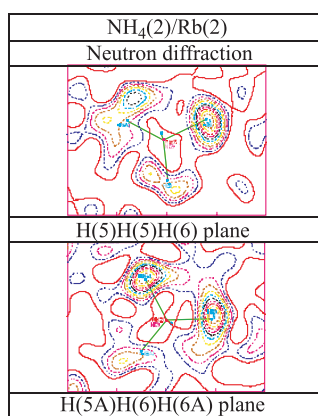


Fig. 8. The Fo-Fc DFM of nuclear density near NH₄(2)/Rb(2) group in HiHkHj planes

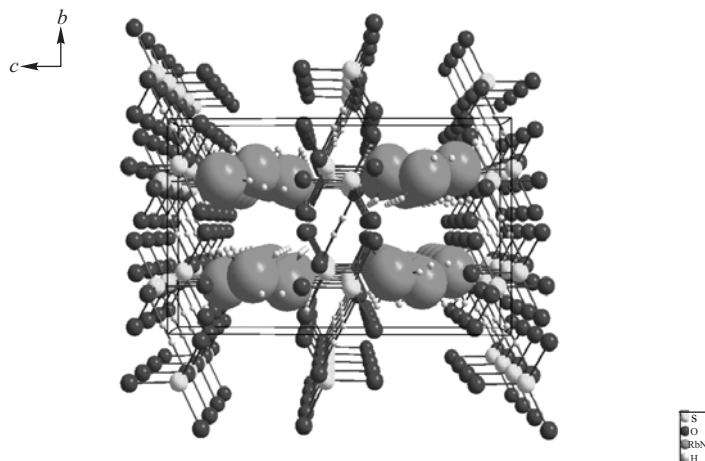


Fig. 9. Projection of crystal structure of the $[\text{Rb}_{0.11}(\text{NH}_4)_{0.89}]_3\text{H}(\text{SO}_4)_2$ mixed crystal along the X axis – direction $[100]$ (phase II at room temperature)

linked to $\text{NH}_4(1)$ ammonium ion. One can see that the maxima for hydrogens usually appear in several maps in the direction perpendicular to the N1_010 plane. The largest variation is observed for H3 that could be also connected with a certain degree of disorder in this direction. The size of contours is smaller for H2. Unfortunately, one can only see the tails of densities for H1 and H4.

A similar presentation of the Fo-Fc DFM of electron density and the Fo-Fc DFM of nuclear density for $\text{NH}_4(2)$ is given in Fig. 6. The zero plane is N2_010 . Then, one can see H5 and the symmetry related to H5a atoms on the planes 0.45 and 0.30 Å below N2_010 zero plane. Both H5 and H5a hydrogen atoms are equivalent and relatively well-defined similar to the H6 and H6a atoms in the planes 0.45 and 0.30 Å above N2_010 zero plane. The H6 atom is better defined and its density is more compact.

The Fo-Fc DFM of electron densities are constructed in the same manner as the Fo-Fc DFM of nuclear densities.

The Fo-Fc DFM of electron charge densities and the Fo-Fc DFM of nuclear densities in the planes of the type HiHjHk ($i, j, k = 1, 2, 3, 4$) of $\text{NH}_4(1)$ and $\text{NH}_4(2)$ ammonium groups are presented in Figs. 7 and 8, respectively. For $\text{NH}_4(1)/\text{Rb}(1)$ group the Fo-Fc DFMs are presented in $\text{H}(1)\text{H}(2)\text{H}(3)$, $\text{H}(2)\text{H}(3)\text{H}(4)$, $\text{H}(3)\text{H}(4)\text{H}(1)$ and $\text{H}(4)\text{H}(1)\text{H}(2)$ planes. The Fo-Fc DFM of electron density near $\text{NH}_4(1)/\text{Rb}(1)$ group have a disposition to form the distribution of the electron density in the form of toroid with local maxima of hydrogen localization.

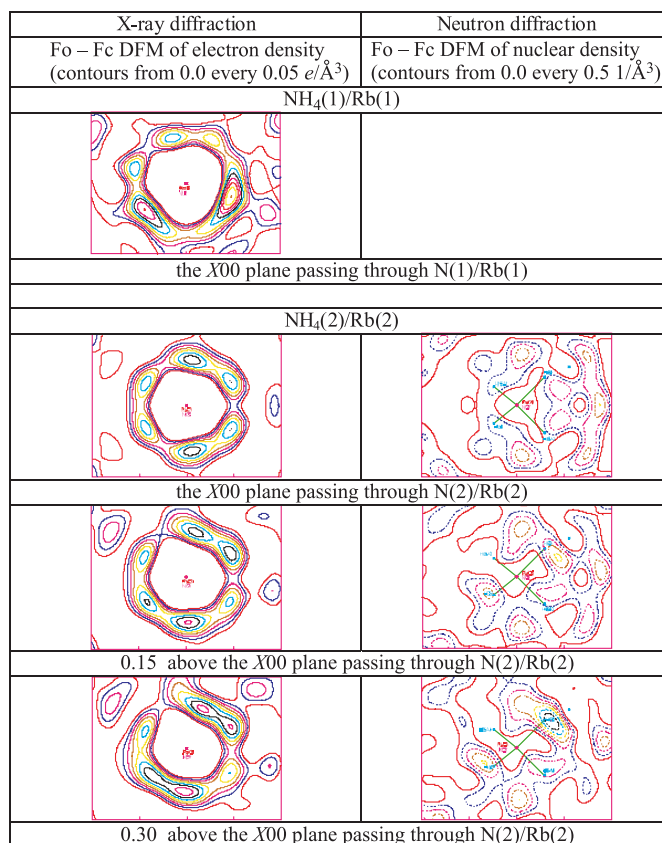


Fig. 10. The Fo-Fc DFM of electron density and nuclear density near NH₄(1)/Rb(1) and NH₄(2)/Rb(2) groups

The Fo-Fc DFM of nuclear densities near NH₄(1)/Rb(1) group show that certain hydrogen atoms localize double positions. A similar situation is observed in Fo-Fc DFM of nuclear densities near NH₄(2)/Rb(2) group in planes H(5)H(5a)H(6) and H(5a)H(6)H(6a).

The projection of crystal structure of the [Rb_{0.11}(NH₄)_{0.89}]₃H(SO₄)₂ mixed crystal along the X-axis, direction [100], is presented in Fig. 9. The Fo-Fc DFM of electron density in the (X00) plane, passing through NH₄(1)/Rb(1) atom, and the Fo-Fc DFM of electron density and the Fo-Fc DFM of nuclear density in the (X00) plane, passing through NH₄(2)/Rb(2) atom and shifted from N(2)/Rb(2) atom on 0.15 and 0.30 Å, respectively, are presented in Fig. 10. The presented

Fo–Fc DFM of electron density point to positions of hydrogen atoms on the toroid.

CONCLUSION

The main conclusion from the study of the $[\text{Rb}_{0.11}(\text{NH}_4)_{0.89}]_3\text{H}(\text{SO}_4)_2$ mixed crystal, carried out by X-ray and neutron single-crystal diffraction, consists in the possibility to present the geometrical form of the ammonium ion in this compound as regular tetrahedron.

Indeed, the results of the study of the inelastic incoherent neutron scattering (IINS) from $(\text{NH}_4)_3\text{H}(\text{SO}_4)_2$ and $[\text{Rb}_{0.18}(\text{NH}_4)_{0.82}]_3\text{H}(\text{SO}_4)_2$ mixed crystal, carried out on the NERA-PR neutron spectrometer on the IBR-2 pulsed reactor (FLNP JINR, Dubna, Russia) at different temperatures (obtained IINS spectra are presented in Fig. 11), show the observation of significant contributions of quasi-elastic incoherent neutron scattering (QINS) to the IINS spectra on the wings of the elastic diffraction line at $\lambda = 4.15 \text{ \AA}$ from crystals-monochromators.

The QINS contributions to the IINS spectra of $(\text{NH}_4)_3\text{H}(\text{SO}_4)_2$ are observed at 290 K in phase II and at 152 K in phase III. The QINS contributions to the IINS

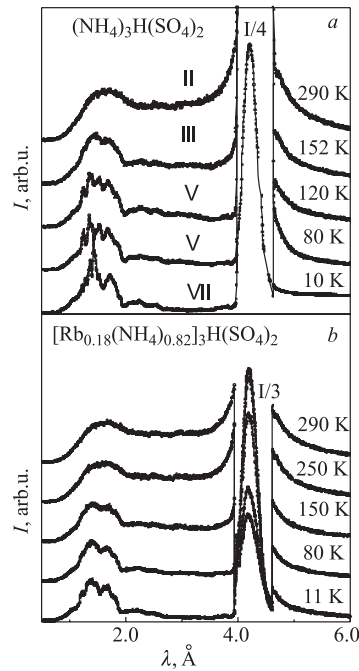


Fig. 11. The inelastic incoherent neutron scattering spectra at different temperatures: a) $(\text{NH}_4)_3\text{H}(\text{SO}_4)_2$ and b) $[\text{Rb}_{0.18}(\text{NH}_4)_{0.82}]_3\text{H}(\text{SO}_4)_2$ mixed crystal

spectra of phases V and VII are not observed at cooling from 120 up to 10 K. The QINS contributions to the IINS spectra of the $[\text{Rb}_{0.18}(\text{NH}_4)_{0.82}]_3\text{H}(\text{SO}_4)_2$ mixed crystal are observed in phase II from 290 to 150 K and further the QINS contributions disappear at cooling from 80 to 11 K.

The observation of QINS contributions to IINS spectra from the $[\text{Rb}_{0.18}(\text{NH}_4)_{0.82}]_3\text{H}(\text{SO}_4)_2$ mixed crystal evidences the possibility of the re-orientation of the ammonium tetrahedra from room temperature up to 150 K. Orientational positions of ammonium ions are determined by the positions of minima of rotational potential and different orientations are separated by U potential barriers. The reorientation of the ammonium groups could be either around molecular symmetry axes of ammonium tetrahedron or around crystallographic symmetry axes. The types of real reorientation within crystal lattice depend on the values of U potential barriers for these different reorientations. In accordance with Frenkel's model [8], ammonium ions can jump over potential barriers amongst different types of the above motion orientations at high temperature, at which thermal excitations of the ammonium ions are close to magnitude of rotational potential.

A probability of reorientation is determined as $1/\tau$, where τ is the average time between two successive jumps. This characteristic time is described by Arrhenius law [9]:

$$\tau = \tau_o \exp(U_a/k_B T), \quad (1)$$

and U_a activation energy is determined as the difference between the height of the U potential barrier and the librational ground state energy, k_B — Boltzmann constant. The probability of the reorientation is decreased at cooling in accordance with Eq. (1) and this is accompanied by decreasing of QINS contribution into the IINS spectrum. Thus, the differential Fourier maps of ammonium groups and the IINS spectra reflect the complex orientational positions of ammonium ions and their possible behaviour within the crystal lattice.

It appears impossible to localize hydrogen atoms from X-ray data even applying numerical absorption correction. The Fo-Fc DFM of electron densities near $\text{NH}_4(1)/\text{Rb}(1)$ and $\text{NH}_4(2)/\text{Rb}(2)$ groups above, in and below the XOZ plane (Figs. 5 and 6), in $\text{H}(1)\text{H}(2)\text{H}(3)$, $\text{H}(2)\text{H}(3)\text{H}(4)$, $\text{H}(3)\text{H}(4)\text{H}(1)$ and $\text{H}(4)\text{H}(1)\text{H}(2)$ planes (Fig. 7), also for $\text{NH}_4(1)/\text{Rb}(1)$ and $\text{NH}_4(2)/\text{Rb}(2)$ group above and in the $XO0$ plane (Fig. 10) show additional maxima. These maxima of electron density could be considered as the disorder of the cations. Alternative explanation of the appearance of additional maxima in electron density may be a wrong estimation of Rb cation amount and in this case one can see residual valence electron density of the Rb cation polarized by the closest environment. One can see from Fo-Fc DFM of electron density that electron density around N/Rb positions is presented by a toroid. Usually, there are several maxima of electron density on the toroid. However, one should keep in mind that the X-ray scattering factor of hydrogen

is by far lower than the scattering factor for non-hydrogens, whereas the neutron scattering lengths of hydrogen and non-hydrogen atoms are comparable, so the neutron data should be more reliable and this is why careful neutron investigations are essential for such systems.

The determination of the anisotropic thermal parameters of hydrogen atoms is possible on the basis of neutron diffraction data. All atomic displacement parameters of hydrogens are relatively large compared to non-H-atoms, as it follows from Table 4, and is demonstrated in Fig. 3. Hydrogen atoms H(1), H(3) and H(5) are segregated significantly due to their thermal ellipsoids. Now it is interesting to analyze the nuclear density distribution of these hydrogen atoms on Fo-Fc DFM of nuclear density for $\text{NH}_4(1)/\text{Rb}(1)$ and $\text{NH}_4(2)/\text{Rb}(2)$ groups.

Indeed, the Fo-Fc DFM of nuclear density distribution for $\text{NH}_4(1)/\text{Rb}(1)$ group shows complex distribution for atoms H(1) and H(3) located on the height 0.45 Å above the XOZ plane passing through N(1)/Rb(1) atom (Fig. 5). Similarly, the Fo-Fc DFM of nuclear density distribution for $\text{NH}_4(2)/\text{Rb}(2)$ group shows complex distribution for atoms H(5), located on the height 0.45 Å below the XOZ plane passing through N(2)/Rb(2). In some cases two separate positions for the selected hydrogens in NH_4^+ cations are possible. This feature may mean that there is a dynamic disorder of NH_4^+ cations in this compound. An alternative explanation is that the real symmetry of this compound is lower than that used in the measurement and refinement. And, in fact, what we observe is the result of averaging in the higher symmetry space group of two slightly different cation positions, which are independent at the real lower symmetry space group.

However, if this is so, some additional weak reflections should be observed during accurate neutron measurements. If they exist, then they could even change the unit cell parameters.

It is interesting to continue the refinement of crystal structures of phases II and III of $(\text{NH}_4)_3\text{H}(\text{SO}_4)_2$ by the X-ray and neutron single-crystal diffraction for the comparison with the results obtained for $[\text{Rb}_{0.11}(\text{NH}_4)_{0.89}]_3(\text{SO}_4)_2$ in order to understand the role of splitted nuclear density maps for some hydrogen atoms of ammonium ions in connection with the observation of QINS contribution in IINS spectra.

REFERENCES

1. Bronowska W., Videnova-Adrabinska V., Pietraszko A. // *Ferroelectrics*. 1995. V. 172. P. 411.
2. Bronowska W., Pietraszko A., Videnova-Adrabinska V. // *Mat. Sci. Forum*. 1993. V. 133–136. P. 727.
3. Baranov A. I. et al. // *Ferroelectrics*. 1998. V. 217. P. 285.

4. *Frontasyeva M. V., Pavlov S. S.* Problems of Modern Physics / Ed. A. N. Sissakian, D. I. Trubetskov. Dubna: JINR, 1999. P. 152–158.
5. *Dominiak P. M., Herold J., Kolodziejcki W., Wozniak K.* // Inorg. Chem. 2003. V. 42. P. 1590.
6. http://www.hmi.de/bensc/instrumentation/pdf_files/BENSC_E5.pdf.
7. *Vainstein B. K.* Modern Crystallography. V. 1. M.: Nauka, 1979 (in Russian).
8. *Frenkel J.* // Acta Phys. Chim. URSS. 1935. V. 3. P. 23.
9. *Bée M.* Quasielastic Neutron Scattering. Bristol and Philadelphia: Adam Hilger, 1988.

Received on April 25, 2006.

Корректор *Т. Е. Понько*

Подписано в печать 17.07.2006.

Формат 60 × 90/16. Бумага офсетная. Печать офсетная.

Усл. печ. л. 1,43. Уч.-изд. л. 2,05. Тираж 295 экз. Заказ № 55410.

Издательский отдел Объединенного института ядерных исследований
141980, г. Дубна, Московская обл., ул. Жолио-Кюри, 6.

E-mail: publish@jinr.ru

www.jinr.ru/publish/